A neutron scattering study of the dilute dipolar-coupled ferromagnets $LiTb_{0.3}Y_{0.7}F_4$ and $LiHo_{0.3}Y_{0.7}F_4$ structure, magnetisation and critical scattering

1989 J. Phys.: Condens. Matter 1 5743

(http://iopscience.iop.org/0953-8984/1/33/019)

J. Phys.: Condens. Matter 1 (1989) 5743–5757. Printed in the UK

A neutron scattering study of the dilute dipolar-coupled ferromagnets $LiTb_{0.3}Y_{0.7}F_4$ and $LiHo_{0.3}Y_{0.7}F_4$. Structure, magnetisation and critical scattering

K Kjaer†, J Als-Nielsen†, I Laursen‡ and F Krebs Larsen

† Risø National Laboratory, DK-4000 Roskilde, Denmark

‡ Technical University, DK-2800 Lyngby, Denmark

§ Århus University, DK-8000 Århus, Denmark

Received 12 August 1988

Abstract. By neutron scattering we have studied the ferromagnetic phase transition in the dilute dipolar-coupled Ising magnets $LiTb_{0.3}Y_{0.7}F_4$ and $LiHo_{0.3}Y_{0.7}F_4$. The Curie temperatures were 0.49 K and 0.36 K, respectively. At low temperatures, the saturation magnetic moment per rare earth ion is only 60% of that observed in the undiluted materials. Just below T_C the singular variation of the magnetisation is consistent with mean-field theory as well as with renormalisation group theories. Above the phase transition, the critical scattering from $LiHo_{0.3}Y_{0.7}F_4$ is strongly asymmetric in Q-space, in agreement with renormalisation group theory. In contrast, the scattering from $LiTb_{0.3}Y_{0.7}F_4$, although also strongly asymmetric, contains an anomalous component at small angles. The saturation magnetisation data are in good agreement with a Monte Carlo simulation study.

1. Introduction

The dipolar-coupled uniaxial ferromagnets $LiRF_4$ [R ≡ Tb or Ho] have been studied by a variety of experimental methods (for $LiTbF_4$, a very complete set of data exists: see Ahlers *et al* 1975, Als-Nielsen 1976, Als-Nielsen *et al* 1975, Griffin *et al* 1977, Fröwein *et al* 1979, Beauvillain *et al* 1980d and Holmes *et al* 1975). The critical behaviour at the ferromagnetic phase transition is in good agreement with a renormalisation group (RG) theory (Larkin and Khmel'nitskii 1969, Aharony and Fisher 1973, Aharony 1973, Aharony and Halperin 1975, Bervillier 1975, Brézin and Zinn-Justin 1976), which predicts mean-field-like critical behaviour with small logarithmic corrections.

Renewed interest in this class of materials was spurred by the theory by Aharony (1976) on site-random Ising dipolar magnets, since such systems can be realised by dilution of the rare earth ions by non-magnetic yttrium ions, i.e., R ≡ Tb_pY_{1-p} or Ho_pY_{1-p}, $p < 1$.

Susceptibility measurements have been reported (Beauvillain *et al* 1980a, b, c, Griffin *et al* 1980a, Folkins 1982) on the diluted magnets $LiTb_pY_{1-p}F_4$, in which the magnetic 4f ions have been diluted by non-magnetic yttrium ions. In contrast with theory (Aharony 1976), a marked departure from mean-field theory was observed in the susceptibility critical exponent γ, which rose well above unity as the concentration p was lowered.

0953-8984/89/335743 + 15 $02.50

Table 1. The (Scheelite) structure of the compounds $LiRF_4$, (R ≡ heavy rare earth ion or yttrium). The origin is at the inversion point. In the body centred cell, there are four formula units, i.e., $Z = 4$.

Ion	Coordinates	Wyckoff Label	Site symmetry
Li^+	$\pm(0\ \frac{1}{4}\ \frac{1}{8})$	4a	$\bar{4}$
R^{3+}	$\pm(0\ \frac{1}{4}\ \frac{5}{8})$	4b	$\bar{4}$
F^-	$\pm(x\ y\ z;$ $\bar{x}\ \frac{1}{2}-y\ z;$ $\frac{3}{4}-y\ \frac{1}{4}+x\ \frac{1}{4}+z;$ $\frac{1}{4}+y\ \frac{1}{4}-x\ \frac{1}{4}+z)$	16f	1

This paper describes neutron scattering studies of $LiTb_{0.3}Y_{0.7}F_4$ and $LiHo_{0.3}Y_{0.7}F_4$. Our results indicate a continuous ferromagnetic transition at $T_C = 0.49$ K ($LiTb_{0.3}Y_{0.7}F_4$) and 0.36 K ($LiHo_{0.3}Y_{0.7}F_4$). Data are presented for the spontaneous magnetisation and the critical scattering, i.e., the wavevector-dependent susceptibility.

In § 2 below, we review some of the necessary information on these systems. In § 3, each experiment reported here is described, and the results are presented. In § 4 we discuss the results and form conclusions.

2. Preliminary information

2.1. Crystal structure

The compounds $LiRF_4$, with R representing a heavy rare earth ion, yttrium or a mixture of these, crystallise in the tetragonal Scheelite structure. The space group is $I4_1/a$. There are four formula units in the centred tetragonal cell, in the positions given in table 1.

Each Li ion is surrounded by a fluorine tetrahedron (with an Li–F distance of 1.90 Å). The rare earth ions are surrounded by two fluorine tetrahedra of different shape (with R–F distances 2.26 and 2.31 Å).

2.2. Magnetic properties

In the crystal field of the Scheelite crystals, the ground state of the Ho^{3+} ion is a doublet, and the excited states, the lowest of which is a singlet 9–10 kelvin higher (Hansen *et al* 1975, Janssen *et al* 1985), can be disregarded for the purposes of this paper. The lowest states of the Tb^{3+} ion are a pair of singlets 1.34 K apart. The higher states are at least 100 K higher (Hansen *et al* 1975). In the ground states, the 4f magnetic moments are parallel to the tetragonal axis: the g-factors are $g_\perp = 0$, $g_\parallel = 13.4$–14.0 in $LiHoF_4$ (Beauvillain *et al* 1978, Magariño *et al* 1980, Janssen *et al* 1985); $g_\perp = 0$, $g_\parallel = 17.7$ in $LiTbF_4$ (Holmes *et al* 1973a, Laursen and Holmes 1974, de Groot *et al* 1981).

For the dilute crystals $LiR_pY_{1-p}F_4$ the same $g_\parallel$ and $g_\perp$ values are found as for the concentrated crystals (Laursen and Holmes 1974, Hansen *et al* 1975, Sattler and Nemarich 1971, Magariño *et al* 1980, Beauvillain *et al* 1980e, Magariño *et al* 1976, Holmes *et al* 1973a, Holmes *et al* 1973b). Thus, the crystal field at a rare earth ion site seems to be independent of the ions present at other rare earth sites.

Ferromagnetism has been observed in $LiTbF_4$ and $LiHoF_4$ (Holmes *et al* 1973a, Als-Nielsen *et al* 1975, Griffin *et al* 1977, Fröwein *et al* 1979, Hansen *et al* 1975†, Cooke *et al* 1975, Battison *et al* 1975, Griffin *et al* 1980b) below Curie points T_C of 2.87 and 1.55 K, respectively. The transitions are continuous. A mean-field theory including only magnetostatic dipolar interactions between the ionic magnetic moments yields Curie–Weiss temperatures that are close to the observed T_C, indicating that exchange contributions to the ordering field are small (for a discussion see, e.g. Kjaer 1984).

3. Experimental procedure and results

3.1. Crystal growth

Crystals of $LiX_pY_{1-p}F_4$, with X ≡ Tb or Ho and $p = 0.30 \pm 0.02$, were grown by a modified Stockbarger technique (Kjaer 1984, Laursen and Holmes 1974). For the holmium compound, ^{7}Li was used to avoid neutron absorption by the (7.5 per cent naturally abundant) ^{6}Li nuclei.

3.2. Structure refinement of $LiTb_{0.3}Y_{0.7}F_4$

A 4 mm single-crystal sphere of $LiTb_{0.3}Y_{0.7}F_4$ was mounted on a four-circle diffractometer, in a monochromatic neutron beam of wavelength $\lambda = 1.070$ Å from the Risø DR3 reactor. At room temperature 1283 reflections and at low temperature (175 K) 1213 reflections were measured within a sphere of $(\sin\theta)/\lambda < 0.79$ Å^{-1}. The resulting integrated intensities were corrected for absorption using the linear absorption coefficient $\mu = 0.70$ cm^{-1}.

Observed structure factors F^2 in arbitrary units were deduced, $F^2 \propto \sin(2\theta) \times$ (integrated intensity), where $\sin(2\theta)$ is the inverse Lorentz factor. Assuming the space group $I4_1/a$, the structure factors were averaged over each set $\{hkl\}$ of symmetry-related reflections, giving about 290 reflections for each temperature and internal consistency factors R_{int} of 2.7%, where

$$R_{\text{int}} = \sum_{hkl} |F^2_{\text{obs}} - \langle F^2_{\text{obs}} \rangle| \Big/ \sum F^2_{\text{obs}}.$$

About 100 reflections that are forbidden in $I4_1/a$ symmetry were measured and found to be zero or only just significant. They were not included in the subsequent refinement.

The observed structure factors F^2_{obs} were compared with the calculated ones

$$F^2_{hkl} = \left| \sum_j b_j \exp(i\boldsymbol{\tau} \cdot \boldsymbol{r}_j) \exp(-\tfrac{1}{2}\boldsymbol{\tau} \cdot \mathbf{U}_j \cdot \boldsymbol{\tau}) \right|^2 \tag{1}$$

where, for atom j at position $\boldsymbol{r}_j$, b_j is the scattering length and the anisotropic thermal vibrations enter through the $\mathbf{U}_j$-matrix. $\boldsymbol{\tau} = h\boldsymbol{a}^* + k\boldsymbol{b}^* + l\boldsymbol{c}^*$ is the Bragg vector, $|\boldsymbol{\tau}| =$

† These authors quote $T_C = 1.30$ K for $LiHoF_4$, in contrast with the value $T_C = 1.50$–1.55 given by most authors.

Table 2. Lattice constants of some Scheelite crystals $LiRF_4$, for various ions R.

R	*a* (Å)	*c* (Å)	*c*/*a*	Temperature (K)
Y[a]	5.175(5)	10.74(1)	2.077	300
Tb[a]	5.200(5)	10.89(1)	2.094	300
Tb[b]	5.192(3)	10.875(6)	2.095	300
Tb[b]	5.181(3)	10.873(6)	2.099	100
Ho[a]	5.175(5)	10.75(1)	2.078	300
Yb[c]	5.1335(2)	10.588(2)	2.063	300
$Ho_{0.3}Y_{0.7}$[d]	5.146(1)	10.758(1)	2.090	1
$Tb_{0.3}Y_{0.7}$[d]	5.18(1)	10.83(1)	2.09	300
$Tb_{0.3}Y_{0.7}$[d]	5.186(5)	10.826(5)	2.087	175
$Tb_{0.3}Y_{0.7}$[d]	5.130(1)	10.735(1)	2.093	1

[a] Keller and Schmutz 1965.
[b] Als-Nielsen *et al* 1975.
[c] Thoma *et al* 1970.
[d] Present work.

$4\pi(\sin\theta)/\lambda$. Starting from the parameters of LiTbF (Als-Nielsen *et al* 1975), the structure of $LiTb_{0.3}Y_{0.7}F_4$ was refined by minimising the expression

$$\sum_{hkl} \sigma_{hkl}^{-2}\left(\frac{F_{\text{obs}}^2}{E_{hkl}} - k^2F_{\text{calc}}^2\right)^2.$$

Here the observed intensities are corrected for extinction by the isotropic factor $E_{hkl}(g)$ which depends on the adjustable parameter g (Becker and Coppens 1974, 1975). k is a scale factor. The standard deviation σ_{hkl} of F_{obs}^2 was based on counting statistics or on the scatter of symmetry-related reflections, whichever yielded the larger value. The structure could be refined within the Scheelite structure with resulting R-factors:

$$R = \sum_{hkl} |F_{\text{obs}}^2 - E_{hkl}k^2F_{hkl}^2| \Big/ \sum F_{\text{obs}}^2$$

of 3.7% and 3.3% for the room temperature and cold data, respectively. The refined extinction parameter g is 4900 ± 150, corresponding to a (Lorentzian) mosaic distribution of width 6.7″ (HWHM). Allowing the individual scattering lengths b_j to vary did not yield significantly lower R-values nor did this change the b_j from their nominal values b(natural lithium) $= -0.214 \times 10^{-12}$ cm, b(Tb) $= b$(Y) $= 0.76 \times 10^{-12}$ cm and b(F) $= 0.56 \times 10^{-12}$ cm (Bacon 1977). The weak reflections were consistently observed to be stronger than the calculated values. A correction for an assumed second-order contamination of the monochromatic beam of 0.5% or 2% did not remedy this discrepancy. Thus we assume that the extra intensity comes from multiple scattering.

In table 2 the lattice constants of the $LiRF_4$ crystals are compared, and table 3 shows the results of this structural analysis and compares it to other known structures.

3.3. Low-temperature measurements

For these measurements the samples were mounted in a ^3He–^4He dilution refrigerator. Controlled temperatures down to 0.090 K were obtained.

Table 3. The known structures of $LiRF_4$ crystals. The temperature parameters U of the $\mathbf{U}_j$ matrix are defined through equation (1).

Compound	Atom	x	y	z	U_{11} (Å^2)	U_{22} (Å^2)	U_{33} (Å^2)	U_{12} (Å^2)	U_{13} (Å^2)	U_{23} (A^2)	Temp-erature	Radiation
$LiTbF_4$[a]	Li	0	$\frac{1}{4}$	$\frac{1}{8}$	0.0202(24)	$=U_{11}$	0.0268(16)	0	0	0	295	1.07 Å
	Tb	0	$\frac{1}{4}$	$\frac{5}{8}$	0.0125(5)	$=U_{11}$	0.0110(3)	0	0	0		neutrons
	F	0.2198(1)	0.4119(1)	0.4560(1)	0.0182(3)	0.0177(3)	0.0172(3)	0.0035(2)	0.0040(2)	0.0030(2)		
	Li	0	$\frac{1}{4}$	$\frac{1}{8}$	0.0163(35)	$=U_{11}$	0.0178(21)	0	0	0	100	
	Tb	0	$\frac{1}{4}$	$\frac{5}{8}$	0.0092(7)	$=U_{11}$	0.0089(4)	0	0	0		
	F	0.2199(2)	0.4107(2)	0.4563(2)	0.0127(4)	0.0124(4)	0.0127(4)	0.0014(4)	0.0016(3)	0.0010(3)		
$LiTb_{0.3}Y_{0.7}F_4$[b]	Li	0	$\frac{1}{4}$	$\frac{1}{8}$	0.0121(5)	$=U_{11}$	0.0165(10)	0	0	0	295	1.07 Å
	Tb/Y	0	$\frac{1}{4}$	$\frac{5}{8}$	0.0054(2)	$=U_{11}$	0.0050(3)	0	0	0		neutrons
	F	0.21887(8)	0.41394(7)	0.45618(4)	0.0104(2)	0.0101(2)	0.0110(2)	−0.0033(1)	0.0039(1)	−0.0029(1)		
	Li	0	$\frac{1}{4}$	$\frac{1}{8}$	0.0086(5)	$=U_{11}$	0.0118(10)	0	0	0	175	
	Tb/Y	0	$\frac{1}{4}$	$\frac{5}{8}$	0.0035(2)	$=U_{11}$	0.0025(3)	0	0	0		
	F	0.21914(8)	0.41329(8)	0.45623(4)	0.0066(2)	0.0066(2)	0.0058(3)	−0.0017(1)	0.0019(1)	−0.0013(1)		
$LiYbF_4$[c]	Li	0	$\frac{1}{4}$	$\frac{1}{8}$	0.020(7)	$=U_{11}$	0.023(15)	0	0	0	Room	Mo Kα x-rays
	Yb	0	$\frac{1}{4}$	$\frac{5}{8}$	0.0073(1)	$=U_{11}$	0.0029(1)	0	0	0		
	F	0.2166(6)	0.4161(6)	0.4564(3)	0.013(1)	0.011(1)	0.008(1)	0.0043(8)	0.0033(9)	0.0028(9)		

[a] Als-Nielsen *et al* 1975.
[b] Present work.
[c] Thoma *et al* 1970.

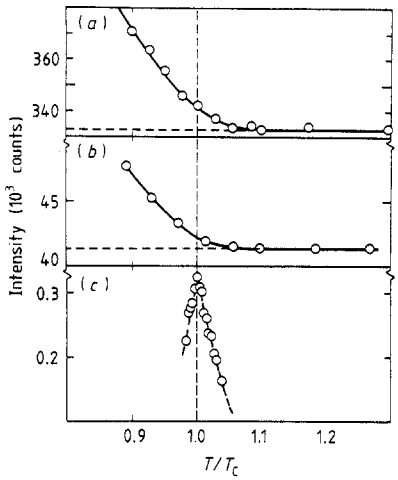

Figure 1. Neutron intensity versus reduced temperature T/T_C. (*a*) (103) Bragg intensity from $LiTb_{0.3}Y_{0.7}F_4$, $T_C = 0.493$ K. (*b*) (103) Bragg intensity from $LiHo_{0.3}Y_{0.7}F_4$, $T_C = 0.360$ K. (*c*) Critical scattering from $LiHo_{0.3}Y_{0.7}F_4$ at $(0.03\,a^*\,0\,0)$, $T_C = 0.360$ K.

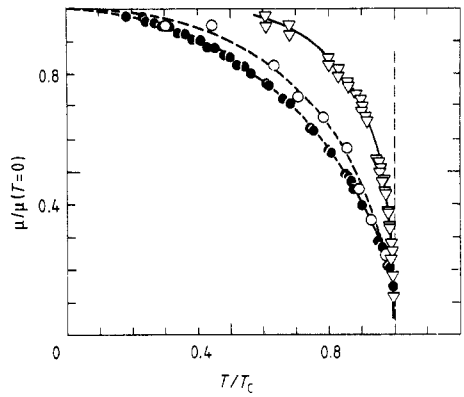

Figure 2. Reduced magnetic moment versus reduced temperature for $LiRF_4$ crystals. ●, R ≡ $Tb_{0.3}Y_{0.7}$; ○, R ≡ $Ho_{0.3}Y_{0.7}$; ▽, R ≡ Tb (from Als-Nielsen *et al* 1975). The lines are guides for the eye.

3.4. Ferromagnetic ordering

This was detected by a continuous increase in the intensity of the magnetic Bragg reflections (103), (301) and (305) (figure 1(*a*) and 1(*b*)). For the holmium compound, a peak in the critical scattering also marked the transition (figure 1(*c*)). The Curie temperatures were 0.49 K for $LiTb_{0.3}Y_{0.7}F_4$ and 0.36 K for $LiHo_{0.3}Y_{0.7}F_4$.

For a ferromagnetic crystal, the elastic neutron cross section at Bragg setting $\boldsymbol{Q} = \boldsymbol{\tau}_{hkl}$ is

$$\frac{d\sigma}{d\Omega} \propto F_{\text{nuc}}^2 + F_{\text{magn}}^2. \tag{2}$$

The nuclear structure factor is given by equation (1), and the magnetic contribution takes the form

$$F_{\text{magn}}^2(\langle\mu\rangle) = \left|\frac{\langle\mu\rangle}{\mu_B}(2.7\text{ fm})f\left(\frac{\sin\theta}{\lambda}\right)\left(1-\frac{\tau_z^2}{\tau^2}\right)^{1/2} p\sum_{j\text{mag}} \exp(i\boldsymbol{\tau}\cdot\boldsymbol{r}_j)\exp(-\tfrac{1}{2}\boldsymbol{\tau}\cdot\mathbf{U}_j\cdot\boldsymbol{\tau})\right|^2. \tag{3}$$

Here $\langle\mu\rangle$ is the magnetic moment per magnetic ion in the crystal, 2.7 fm is the magnetic scattering length per Bohr magneton, f is the magnetic form factor†, $(1-\tau_z^2/\tau^2)^{1/2}$ is the polarisation factor, the sum is the geometrical structure amplitude of the R^{3+} sites and p is the fraction of spins present.

† For the low-order reflections used in this study ($(\sin\theta)/\lambda \leqslant 0.37$), the form factor is known quite accurately. The values calculated by Stassis *et al* (1977) for the free, tripositive ions were used.

Table 4. Low-temperature magnetic moments. The μ-values for $LiHoF_4$ are from g-factor measurements and from the saturation magnetisation in a field.

	T_C (K)	hkl	$\lvert F_{nuc}\rvert^2$ (10^{-24} cm^2)	$\mu(T=0)$ (μ_B)	$T_C/T_C(p=1)$	$\mu(T=0)/\mu(T=0, p=1)$
$LiTb_{0.3}Y_{0.7}F_4$[a]	0.49	103	(0.212)	(3.6)		
($p = 0.3$)		301	2.53	5.0 ± 0.7	0.17	0.56 ± 0.08
$LiTbF_4$[b]	2.87	301	—	8.9		
($p = 1$)		400	—	—		
$LiHo_{0.3}Y_{0.7}F_4$[a]	0.36	103	0.359	—		
($p = 0.3$)		301	2.99	4.6 ± 0.7		
		305	1.03	—	0.23	0.67 ± 0.10
$LiHoF_4$[c,d,e]	1.55	—	—	6.7–7.0		
($p = 1$)		—	—	—		

[a] Present work.
[b] Als-Nielsen *et al* 1975.
[c] Hansen *et al* 1975.
[d] Cooke *et al* 1975.
[e] Battison *et al* 1975.

It follows from equations (2) and (3) that the magnetisation may be found by measurement of the Bragg intensity above and below T_C,

$$\langle\mu\rangle_T/\mu_B = c(I_{nuc+mag}(T)/I_{nuc}(T > T_C) - 1)^{1/2}. \tag{4}$$

This was done for $LiTb_{0.3}Y_{0.7}F_4$ using 13.9 meV neutrons and the (103) and (301) reflections. Consistent results were obtained with increasing and decreasing temperature, and the data from the two reflections could be scaled to fall on the same curve. The magnetisation of the $LiHo_{0.3}Y_{0.7}F_4$ crystal was studied as well, using 15.7 meV neutrons and the (103) reflection. Here, because of longer equilibrium times, the rocking curve was measured many times at each mixer temperature setting until a constant intensity was obtained. Some raw data are shown in figures 1(*a*) and 1(*b*), and figure 2 compares the magnetisation data with those for $LiTbF_4$ (Als-Nielsen *et al* 1975). Apparent in the figure is the very slow saturation in the diluted crystals.

The data in figure 2 have been corrected for critical scattering, assuming that the critical scattering intensities are equal at $(T_C + \Delta T) > T_C$ and $(T_C - \frac{1}{2}\Delta T)$†. The values of the magnetisation critical exponent β are 0.47 ± 0.02 (Tb compound) and 0.48 ± 0.03 (Ho compound).

Absolute values of the magnetic moment may also be derived, since the scale factor c of equation (4) can be calculated

$$c = |F_{nuc}|/|F_{magn}(\langle\mu\rangle = 1\mu_B)|. \tag{5}$$

In table 4 the resulting magnetisations are given and compared with the data for the undiluted crystals.

We now discuss possible sources of error and uncertainty in the results presented in table 4:

† This is the prediction of mean-field theory and was found to apply for $LiTbF_4$ (Holmes *et al* 1975).

(i) At $T \leqslant 1$ K the thermal displacements ($\mathbf{U}_j$) are not known. However, since equation (5) involves a ratio of structure factors, the precise values of the $\mathbf{U}_j$ are not very important; since calculations show that a scatter of not more than $\pm 5\%$ in the resulting magnetic moment $\mu(T = 0)$ results from the use of (i) the 175 K $\mathbf{U}_j$-values, (ii) $\mathbf{U}_j \equiv 0$ or (iii) $\mathbf{U}_j$ extrapolated to zero temperature assuming a Debye-type variation. In table 4, $\mathbf{U}_j \equiv 0$ was used for simplicity.

(ii) Also, the precise fluorine positions are not known for $LiTb_{0.3}Y_{0.7}F_4$ at $T < 1$ K or for $LiHo_{0.3}Y_{0.7}F_4$. Again, a scatter of $\pm 5\%$ in the resulting low-temperature magnetic moments results from the use of various sets of fluorine positions taken from table 3. In table 4 the fluorine positions of $LiTb_{0.3}Y_{0.7}F_4$ at 175 K were used.

(iii) The extinction correction is not known for the samples used in the low-temperature measurements. However, based on the extinction corrections refined for the spherical $LiTb_{0.3}Y_{0.7}F_4$ sample at 175 K, we estimate that the extinction correction probably amounts to not more than 15% in the resulting $\mu(T = 0)$.

(iv) The scatter in the intensity data and the resulting uncertainty in the extrapolation to zero temperature also have to be considered.

The errors quoted in table 4 include all of these sources.

We also comment that the weak nuclear reflections give a large uncertainty in the scale factor c. This is believed to be the cause of the 30% difference between the $Tb_{0.3}Y_{0.7}F_4$ magnetic moments determined from the (103) reflection from that determined from the (301) reflection. Indeed, a calculation based on the *observed* (103) structure factor gives agreement with the (301) datum point, which we consider to be more reliable because its structure factor was determined accurately and consistently in the structure analysis.

For $Ho_{0.3}Y_{0.7}F_4$, the (103) reflection was measured against temperature, and at a few selected temperatures, the (301) and (305) reflections were measured in order to check the scale of the magnetisation.

Thus, for both crystals, the magnetic moment per ion at low temperatures is only about 60% of that observed in the undiluted crystals. Mean-field theory (MF) predicts 100% for the holmium ions which have a doublet ground state. An explanation of the observed effect in terms of frustration effects for the dipolar interaction is given by Knak Jensen and Kjaer (1988).

A small depression of the low temperature magnetic moment (to about 80%†) is predicted by MF for the Tb ions because their split ground state becomes more important as the mean field is lowered in proportion to the Tb concentration. Work is in progress (Knak Jensen 1989) on a Monte Carlo simulation of the diluted dipolar, split ground state system of $LiTb_{0.3}Y_{0.7}F_4$.

3.5. Critical magnetic scattering

This was measured by double-axis neutron diffractometry. Near a second-order phase transition the scattering will be almost purely elastic (Stanley 1971) and the intensity measured by a two-axis neutron diffractometer will be to a good approximation

† A mean field theory of magnets with a split ground state was given by Bleaney (1963). Based on this theory, numerical calculations and plots are given in appendix B of Kjaer (1984). The magnetisation depression is given by $\mu(T = 0)/\mu_{max} = [1 - (\Delta/2k\theta)^2]^{1/2} = 0.78$ for the parameters of $LiTb_{0.3}Y_{0.7}F_4$: the ground state splitting $\Delta/k_B = 1.34$ K (Laursen and Holmes 1974) and the Curie–Weiss temperature $\theta = 0.3 \times 3.6$ K (Holmes *et al* 1973a).

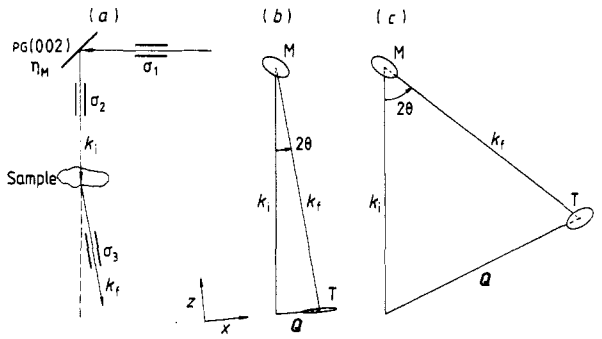

Figure 3. (*a*) Double-axis diffractometer in real space. η_M is the mosaicity of the (pyrolytic graphite (PG)) monochromator crystal, and σ_1–σ_3 are angular collimations. (*b*) Small-angle, and (*c*) large-angle scattering triangles for the sample. After the monochromatisation, the neutrons have a spread in energy and direction (contours M). Assuming elastic scattering by the sample, the resulting $\boldsymbol{Q}$-resolution (contours T) is very much compressed in the small-angle case (*b*). In the calculation, the parameters of line two in table 5 below were used. The resolution contours are shown ×25 expanded relative to the scattering triangle.

$$\frac{d\sigma}{d\Omega} = \int d\omega \frac{d\sigma}{d\Omega\, d\omega} \propto (1 - Q_z^2/Q^2)S(\boldsymbol{Q}) \tag{6}$$

where $S(\boldsymbol{Q})$ is the Fourier-transformed spin–spin correlation function

$$S(\boldsymbol{Q}) \propto \sum_{r,r'} \exp[i\boldsymbol{Q}\cdot(\boldsymbol{r}' - \boldsymbol{r})]\langle \hat{S}^z(\boldsymbol{r}, t=0)\hat{S}^z(\boldsymbol{r}', t=0)\rangle_T \tag{7}$$

$S(\boldsymbol{Q})$ was derived for the paramagnetic phase within mean-field theory (MF) by Holmes *et al* (1975) (see also Kjaer 1984). The result for $(Q_x, Q_y) \gg Q_z$ is

$$S(\boldsymbol{Q}) \propto \frac{\chi_T(\boldsymbol{Q})}{\chi_T^0} \propto \frac{\sigma_0}{1 + \xi^2[|\boldsymbol{Q}|^2 + g(Q_z/Q)^2]} \tag{8}$$

Here $\chi_T(\boldsymbol{Q})$ is the wavevector-dependent magnetic susceptibility and $\chi_T^0 \propto 1/T$ is the single-ion susceptibility in the crystal. The correlation length ξ and the susceptibility σ_0 diverge near T_C according to power laws

$$\xi = [(T - T_C)/T_C]^{-\nu} \qquad \nu_{MF} = \tfrac{1}{2} \tag{9}$$

$$\sigma_0 \propto [(T - T_C)/T]^{-\gamma} \qquad \gamma_{MF} = 1. \tag{10}$$

The parameter g describes the asymmetry of the dipolar interaction between the Ising spins in the tetragonal crystal structure and makes the cross section (8) strongly asymmetric: while its width along Q_x is $1/\xi$, the extent in the Q_z direction is $\sim 1/\xi_\parallel$, where $\xi_\parallel \equiv g^{1/2}\xi^2$. Thus, $S(\boldsymbol{Q})$ approaches the shape of a pancake as $T \to T_C$. MF predicts $g \simeq 1.6$ Å^{-2}.

As shown by Als-Nielsen (1976), a matching resolution can be obtained (in the case of elastic scattering) by measuring $\chi_T(\boldsymbol{Q})$ near the (000) Bragg point.

Table 5. Instrument parameters in the critical scattering measurements. η_M and σ_1–σ_3 are defined in figure 3, and R_x, R_y and R_z are the calculated dimensions (FWHM) of the resolution function. R_z is proportional to the scattering vector $\boldsymbol{Q}$. The calculated R_x values (Møller *et al* 1969, 1970) were in good agreement with the measured widths of the direct beam.

	Monochromator	η_M	k (Å^{-1})	E (meV)	σ_1	σ_2	σ_3	R_x (Å^{-1})	R_y (Å^{-1})	R_z/Q
$LiTb_{0.3}Y_{0.7}F_4$ TAS VI	PG(002) (flat)	30′	1.55	5.02	30′	10′	10′	0.0070	0.05	0.0023
$^7LiHo_{0.3}Y_{0.7}F_4$ TAS VII	PG(002) (flat)	30′	1.14	2.71	32′	14.4′	13.5′	0.0066	0.05	0.0029

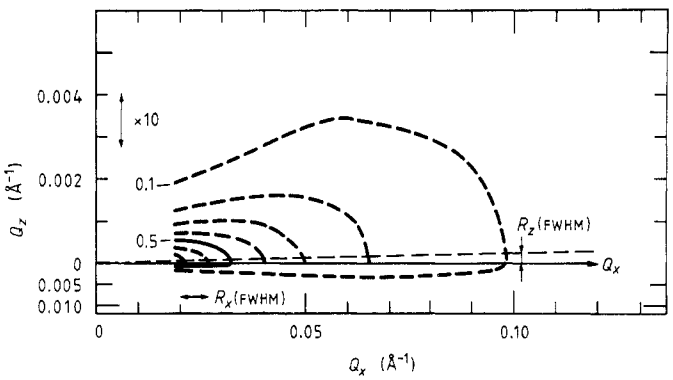

Figure 4. Critical scattering from $^7LiHo_{0.3}Y_{0.7}F_4$ at 1.4% above $T_C = 0.360$ K. The intensity is normalised by the maximum intensity I_0, obtained by extrapolation along the Q_x axis to $Q = 0$. Contour lines are shown for $I/I_0 = 0.1$ to 0.7 in steps of 0.1. Note the ×10 enlargement of the Q_z-scale in the upper part of the figure. Also shown are the calculated resolution widths $R_z \propto Q$ and R_y.

Figure 3 and table 5 give details of the diffractometer and resolution.

3.6. Critical scattering from $LiHo_{0.3}Y_{0.7}F_4$

Figure 4 shows data for $LiHo_{0.3}Y_{0.7}F_4$ just above T_C.

As seen in the figure, the scattering is highly anisotropic. To compare the data with the dipolar cross section, equations (6)–(8), we need to convolve the cross section with the resolution function (Table 5), i.e.

$$I(\boldsymbol{Q}) = \int \mathrm{d}^3\boldsymbol{Q}' \cdot R(\boldsymbol{Q} - \boldsymbol{Q}') \cdot \frac{\mathrm{d}\sigma}{\mathrm{d}\Omega}(\boldsymbol{Q}'). \tag{11}$$

In fact, only the out-of-plane resolution R_y needs to be taken into account (c.f. figure 4 and table 5), reducing (11) to a one-dimensional integral.

By fitting equation (11) to intensities measured at $Q_z = 0$ we have extracted the correlation length ξ and the amplitude σ_0. Subsequently, by fitting (11) to full two-dimensional intensity distributions we have extracted values for the parameter g.

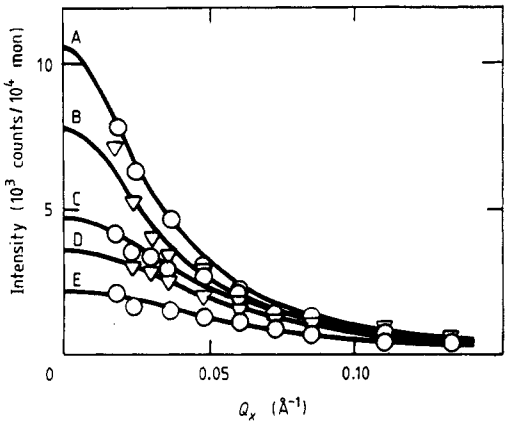

Figure 5. Measured critical scattering $I(Q_x, 0)$ from $^7LiHo_{0.3}Y_{0.7}F_4$ at temperatures T = 0.3650 K (curve A), 0.3674 K (curve B), 0.3705 K (curve C), 0.3733 K (curve D) and 0.3824 K (curve E). The full curves are the best fits of the Lorentzian cross section (8) convolved with the vertical resolution (11).

3.7. On-axis data

Scans were made along the Q_x axis for several temperature settings. Figure 5 shows some of the data.

As seen in the figure, the line shape (11) fits the data quite well. The resulting chi-squared (χ^2) for the fits are in the range 0.7–1.7, and the correlation length ξ and the extrapolated ($Q \rightarrow 0$) cross section σ_0 may be extracted.

3.8. Two-dimensional data

The fingerprint of the dipolar cross section (8) is the peculiar variation with Q_z. Full $I(Q_x, Q_z)$ intensity profiles were measured at two temperatures above T_C. Figure 6 shows again the data represented in figure 4 (T = 0.3650 K). Keeping σ_0 and ξ fixed at the values derived from a $Q_z = 0$ cut in the data, the only adjustable parameter in (8) is the asymmetry parameter g. By fitting only g, the data are well represented by the dipolar cross section.

One more data set $I(Q_x, Q_z)$ was obtained at a higher temperature (0.3824 K, not shown). The results of the fits are given in table 6.

g is changed somewhat from the mean-field value as the phase transition is approached. The good fits of the dipolar cross section to the data lead us to conclude that for $LiHo_{0.3}Y_{0.7}F_4$, the dipolar interaction between the spins is dominant and that the random dilution by the nonmagnetic yttrium ions has not changed the critical behaviour from that of the pure crystal, other than by reducing the transition temperature.

The correlation length and peak intensity follow the power laws of equations (9) and (10) with parameters $\xi_0 = 1.17$, $\nu = 0.59 \pm 0.02$ and $\gamma = 1.38 \pm 0.10$.

3.9. Critical scattering from $LiTb_{0.3}Y_{0.7}F_4$

Figure 7 shows scattering data for $LiTb_{0.3}Y_{0.7}F_4$ just above T_C. As for $LiHo_{0.3}Y_{0.7}F_4$, the scattering is highly anisotropic. However, near the forward direction, for momentum

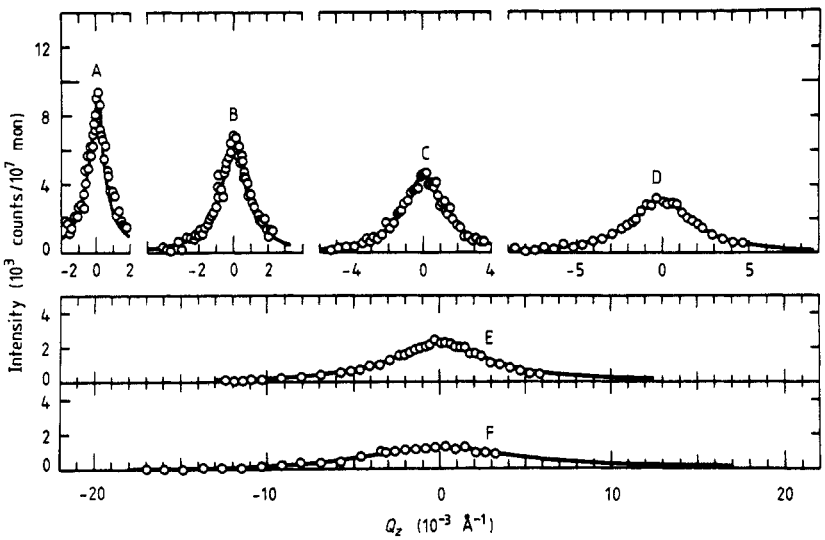

Figure 6. Critical scattering $I(Q_x, Q_z)$ from $^7LiHo_{0.3}Y_{0.7}F_4$ at 0.3650 K $\simeq T_C \times 1.014$ (○). The full curves are a simultaneous fit of equations (8) and (11) to all the data points, allowing only the asymmetry parameter g to vary. Curve A, $Q_x = 0.019$ Å^{-1}; curve B, $Q_x = 0.025$ Å^{-1}; curve C, $Q_x = 0.037$ Å^{-1}; curve D, $Q_x = 0.049$ Å^{-1}; curve E, $Q_x = 0.061$ Å^{-1}; curve F, $Q_x = 0.085$ Å^{-1}.

Table 6. Results of fitting equation (11) to the measured critical scattering $I(Q_x, Q_z)$ from $^7LiHo_{0.3}Y_{0.7}F_4$.

T (K)	$(T - T_C)/T_C$	g (Å^{-2})	Number of points	χ^2
0.3650	1.4%	1.92 ± 0.3	250	2.1
0.3824	6.2%	1.86 ± 0.10	54	1.6
	Mean field	1.57	—	—

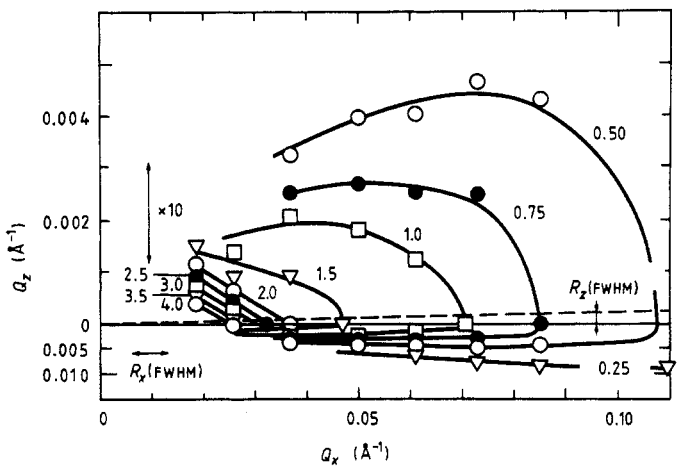

Figure 7. Scattering $I(Q_x, Q_z)$ from $LiTb_{0.3}Y_{0.7}F_4$, at $T = 0.500$ K $\simeq 1.014 \times T_C$. Intensity, represented by contour lines, is in units of counts s^{-1}. Note the ×10 enlargement of the Q_z scale in the upper part of the figure. Also shown are the calculated resolution widths (FWHM) $R_z \propto Q$ and R_x.

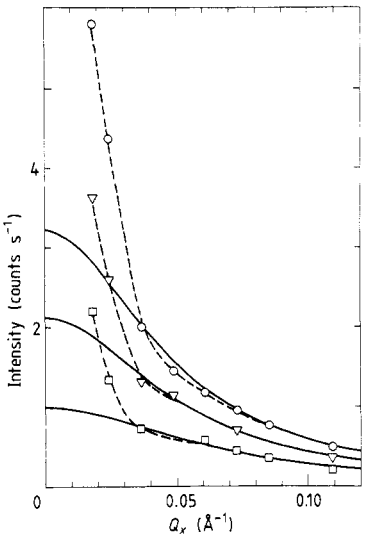

Figure 8. Scattering $I(Q_x, 0)$ from $LiTb_{0.3}Y_{0.7}F_4$ in the paramagnetic phase: ○, 0.500 K ≃ 1.014 × T_C; ▽, 0.530 K ≃ 1.975 × T_C; □, 0.570 K ≃ 1.16 × T_C. Full curves are fits of Lorentzians (no resolution correction). Broken curves are guides to the eye.

transfers $Q_x < 0.03$ Å^{-1}, a sharp rise in the intensity is seen above that predicted by the cross section (8). Qualitatively similar features were observed at two higher temperatures. This is seen more clearly in figure 8 which represents data obtained *on-axis*, $I(Q_x, 0)$.

In figure 8, the full curves are fits of simple Lorentzians, effectively representing the cross section (8) convolved with the vertical resolution. The extra intensity observed at low momentum transfers is indicated by the broken curves, these being guides to the eye. The background (subtracted in the figure) was measured at high temperatures $T \simeq 2T_C$ and was of the order of 70–100% of the resulting signal close to T_C (uppermost curve in figure 8) for all momentum transfers. Errors in the background subtraction are estimated to be of the order of 15% for low momentum transfers $Q_x \simeq 0.02$ Å^{-1} and less for the higher scattering angles.

The measured intensities in figure 8 obviously cannot be extrapolated to zero momentum transfer to give the susceptibility and the correlation length. If an extrapolation is made on the basis of the data for larger momentum transfers $Q_x > 0.03$ Å^{-1} (the (full curve) Lorentzians in the figure), the resulting susceptibilities vary by only a factor of 3 and the correlation length ξ varies only from 16 to 21 Å on going from 16% to 1.4% in reduced temperature $(T - T_C)/T_C$. A correction for the vertical resolution would not change this conclusion significantly.

The scattering was followed as a function of temperature above and below T_C at constant momentum transfers Q_x. A steady increase of intensity was observed even below T_C, no feature marking the transition point. For comparison, a significant peak at T_C was seen in the scattering from $LiHo_{0.3}Y_{0.7}F_4$ (figure 1(*c*)) and $LiTbF_4$ (Als-Nielsen 1976). In $LiTbF_4$, the intensity $I(T)$ rose again when the temperature was lowered below about 0.99 T_C. This effect was attributed to scattering from magnetic domains and was seen to vanish in modest magnetic fields (Møllenbach 1980). To check whether the observed scattering below T_C could be attributed to magnetic domains, we applied a

field along the c axis. For the obtainable fields of 0.05–0.07 T or less, no qualitative change in $I(T)$ was observed. As this applied field would be sufficient to produce a non-zero internal field for magnetisations of 1 Bohr magneton per magnetic ion present, we conclude that magnetic domain scattering is not the source of the rising intensity below T_C.

4. Discussion and conclusion

By a comparison of nuclear and magnetic Bragg scattering of unpolarised neutrons, the spontaneous magnetisation in $LiHo_{0.3}Y_{0.7}F_4$ and $LiTb_{0.3}Y_{0.7}F_4$ has been measured as a function of temperature. The magnetisation saturates slower than predicted by mean field theory, in contrast to the behaviour observed in $LiTbF_4$ (Als-Nielsen *et al* 1975).

The magnetic moment per ion at low temperatures is less than that observed in the undiluted crystals. Thus

$$\langle\mu\rangle(\text{low } T, LiHo_{0.3}Y_{0.7}F_4)/\langle\mu\rangle(\text{low } T, LiHoF_4) = 0.67$$

in good agreement with Monte Carlo simulations (Knak Jensen and Kjaer 1989) which establish frustration effects in the dipolar interaction as the cause of the magnetic moment depression. The larger depression

$$\langle\mu\rangle(\text{low } T, LiTb_{0.3}Y_{0.7}F_4)/\langle\mu\rangle(\text{low } T, LiTbF_4) = 0.56$$

can be intuitively understood as the combined effect of the ground state splitting of the Tb ions and the above-mentioned frustration effect. Work is in progress (Knak Jensen 1989) to extend the Monte Carlo simulations to the Tb system.

The critical exponents β for the spontaneous magnetisation, respectively $\beta = 0.48 \pm 0.03$ and $\beta = 0.47 \pm 0.02$ for the Ho and Tb compounds do not significantly deviate from the mean field (MF) value $\beta = \frac{1}{2}$. The data, however, do not rule out the small modifications to MF predicted by renormalisation group (RG) theories (Larkin and Khmel'nitskii 1969, Aharony and Fisher 1973, Aharony 1973, Bervillier 1975, Brézin and Zinn-Justin 1976, Aharony 1976).

The critical scattering from $LiHo_{0.3}Y_{0.7}F_4$ above T_C is in good agreement with the cross section (8) predicted by MF and RG theories. The asymmetry parameter $g = 1.9$ deviates slightly from the mean field value $g_{MF} = 1.6$. The critical exponent for the correlation length is $\nu = 0.59 \pm 0.02$, but the quality of the data does not permit us to rule out the theoretical predictions (Larkin and Khmel'nitskii 1969, Aharony and Fisher 1973, Aharony 1973, Bervillier 1975, Brézin and Zinn-Justin 1976, Aharony 1976) of a mean-field-like critical behaviour with weak correction factors. The susceptibility diverges according to the power law $\Delta T^{-\gamma}$ with $\gamma = 1.38 \pm 0.10$, deviating significantly from any mean-field-like form.

The critical scattering from $LiTb_{0.3}Y_{0.7}F_4$ is dominated by a component which rises strongly towards $\boldsymbol{Q}_x = 0$, rendering the assignment of correlation lengths ξ and susceptibility σ_0 impossible.

Thus, in conclusion, the magnetisation in both compounds seems well understood. Also, the critical scattering displays the pronounced asymmetry characteristic of the dipolar interaction. The detailed cross section for $LiHo_{0.3}Y_{0.7}F_4$ agrees well with the theoretical expression (8), albeit with slightly renormalised parameters and critical exponents. In contrast, the anomalous low-Q component in the scattering from $LiTb_{0.3}Y_{0.7}F_4$ deviates strongly from the form (8).

Acknowledgments

It is a pleasure to acknowledge helpful discussions with Drs P Bak and A Aharony.

References

Aharony A 1973 *Phys. Rev.* B **8** 3363–70
—— 1976 *Phys. Rev.* B **13** 2092–98
Aharony A and Fisher M E 1973 *Phys. Rev.* B **8** 3323–41
Aharony A and Halperin B I 1975 *Phys. Rev. Lett.* **35** 1308–10
Ahlers G, Kornblit A and Guggenheim H J 1975 *Phys. Rev. Lett.* **34** 1227–30
Als-Nielsen J 1976 *Phys. Rev. Lett.* **37** 1161–4
Als-Nielsen J, Holmes L M, Krebs Larsen F and Guggenheim H J 1975 *Phys. Rev.* B **12** 191–7
Bacon G E 1977 *Neutron Diffraction Newsletter* ed. W B Yelon (Neutron Diffraction Commission, International Union of Crystallography)
Battison J E, Kasten A, Leask M J M, Lowry J B and Wanklyn B M 1975 *J. Phys. C: Solid State Phys.* **8** 4089–5
Beauvillain P, Chappert C and Laursen I 1980d *J. Phys. C: Solid State Phys.* **13** 1481–91
Beauvillain P, Chappert C, Renard J P and Griffin J A 1980b *J. Phys. C: Solid State Phys.* **13** 395–401
Beauvillain P, Chappert C, Renard J P, Griffin J A and Laursen I 1980a *J. Magn. Magn. Mater.* **15–18** 421–3
Beauvillain P, Renard J-P, Laursen I and Walker P J 1978 *Phys. Rev.* B **18** 3360–8
—— 1978 *J. Phys. Coll.* **39** C6 745–6
Beauvillain P, Renard J P and Magariño J 1980e *J. Magn. Magn. Mater.* **15–18** 31–2
Beauvillain P, Seiden J and Laursen I 1980c *Phys. Rev. Lett.* **45** 1362–5
Becker P J and Coppens P 1974 *Acta Crystallogr.* A **30** 129–53
Becker P J and Coppens P 1975 *Acta Crystallogr.* A **31** 417–25
Bervillier C 1975 *J. Physique Lett.* **36** 225–28
Bleaney B 1963 *Proc. R. Soc.* A **276** 19–38
Brézin E and Zinn-Justin J 1976 *Phys. Rev.* B **13** 251–54
Cooke A H, Jones D A, Silva J F A and Wells M R 1975 *J. Phys. C: Solid State Phys.* **8** 4083–8
de Groot P, Leempoels F, Witters J, Herlach F and Laursen I 1981 *Solid State Commun.* **37** 681–3
Folkins J J, Griffin J A and Gubser D U 1982 *Phys. Rev.* B **25** 405–16
Fröwein R, Kötzler J and Assmus W 1979 *Phys. Rev. Lett.* **42** 739–42
Griffin J A, Folkins J J and Gabbe D 1980a *Phys. Rev. Lett.* **45** 1887–90
Griffin J A, Huster M and Folweiler R J 1980b *Phys. Rev.* B **22** 4370–8
Griffin J A, Litster J D and Linz A 1977 *Phys. Rev. Lett.* **38** 251–4
Hansen P E, Johansson T and Nevald R 1975 *Phys. Rev.* B **12** 5315–24
Holmes L M, Als-Nielsen J and Guggenheim H J 1975 *Phys. Rev.* B **12** 180–90
Holmes L M, Guggenheim H J and Als-Nielsen J 1973b *Proc. Int. Conf. Magnetism ICM-73, Moscow* vol. 6 p 256–61
Holmes L M, Johansson T and Guggenheim H J 1973a *Solid State Commun.* **12** 993–7
Janssen P, de Wolf I and Laursen I 1985 *J. Phys. Chem. Solids* **46** 1387–91
Keller C and Schmutz H 1965 *J. Inorg. Nucl. Chem.* **27** 900–1
Kjaer K 1984 *Risø National Laboratory Report* R-506
Knak Jensen S 1989 unpublished
Knak Jensen S and Kjaer K 1989 *J. Phys.: Condens. Matter.* **1** 2361–8
Larkin A I and Khmel'nitskii D E 1969 *Zh. Eksp. Teor. Fiz.* **56** 2087–98 (English translation: *Sov. Phys.–JETP* **29** 1123–8)
Laursen I and Holmes L M 1974 *J. Phys. C: Solid State Phys.* **7** 3765–9
Magariño J, Tuchendler J, Beauvillain P and Laursen I 1980 *Phys. Rev.* B **21** 18–28
Magariño J, Tuchendler J, D'Haenens J P and Linz A 1976 *Phys. Rev.* B **13** 2805–8
Møllenbach K 1980 *Risø National Laboratory Report* R-396
Møller H, Bjerrum and Nielsen M 1969 *Acta Crystallogr.* A **25** 547–50
Møller H, Bjerrum and Nielsen M 1970 *Instrumentation for Neutron Inelastic Scattering Research* (Vienna: IAEA) p 49–71
Sattler J P and Nemarich J 1971 *Phys. Rev.* B **4** 1–5
Stanley H E 1971 *Introduction to phase transitions and critical phenomena* (Oxford: Oxford University Press) p 308
Stassis C, Deckman H W, Harmon B N, Desclaux J P and Freeman A J 1977 *Phys. Rev.* B **15** 369–76
Thoma R E, Brunton G D, Penneman R A and Keenan T K 1970 *Inorg. Chem.* **9** 1096–1101